Electronic Supplementary Information

Single-atomic rhenium-assisted 2H-to-1T phase transformation of MoS_2 nanosheets boosting electrocatalytic hydrogen evolution

Jianmin Yu,[a,c†] Yongteng Qian,[d†] Qing Wang,[a] Chenliang Su,[c] Hyoyoung Lee,[e,f,*] Lu Shang,[a,*] Tierui Zhang[a,b,*]

[a]Key Laboratory of Photochemical Conversion and Optoelectronic Materials, Technical Institute of Physics and Chemistry, Chinese Academy of Sciences, Beijing 100190, China.

[b]Center of Materials Science and Optoelectronics Engineering, University of Chinese Academy of Sciences, Beijing 100049, China

[c]International Collaborative Laboratory of 2D Materials for Optoelectronic Science and Technology of Ministry of Education, Institute of Microscale Optoelectronics, Shenzhen University, Shen Zhen, 518060, China

[d]Department of Physics and Interdisciplinary Course of Physics and Chemistry, Sungkyunkwan University (SKKU), Suwon 16419, Republic of Korea

[e]Center for Integrated Nanostructure Physics, Institute for Basic Science (IBS), Sungkyunkwan University, Suwon, 16419, Republic of Korea

[f]Department of Chemistry, Sungkyunkwan University (SKKU), Suwon 16419, Republic of Korea

[†]These authors contributed equally to this work.

Experimental section

Reagents and materials

All chemicals used in this work as received without further purification. Ammonium perrhenate (NH_4ReO_4; Sigma-Aldrich, ≥99.99%), sodium molybdate dehydrate ($MoNa_2O_4 \cdot 2H_2O$; Sigma-Aldrich, ≥99%), thiourea (NH_2SCNH_2; Alfa Aesar, ≥99%), potassium hydroxide (KOH; Sigma-Aldrich, 85%), sulfuric acid (H_2SO_4; Sigma-Aldrich, ≥99.99%), ethanol (C_2H_5OH; Sigma-Aldrich, ≥99.9%), Pt/C (20 wt % Pt on Vulcan XC-72R, Sigma-Aldrich), Toray carbon cloth (CC, Alfa Aesar).

Synthesis of the Re-SA/MoS_2 electrocatalysts

The Re-SA/MoS_2 electrocatalysts were prepared by a simple one-pot hydrothermal method. To optimize the catalytic activity of the samples, we fabricated a series of Re-SA/MoS_2 catalysts by tuning the molar ratios of Re and Mo ions (0.15:1, 0.20:1, and 0.25:1). The typical synthesis procedure of Re-SA/MoS_2 (Re: Mo = 0.20:1) was used as follows: 0.20 mmol NH_4ReO_4, 1 mmol $MoNa_2O_4 \cdot 2H_2O$, and 2.5 mmol NH_2SCNH_2 were mixed in 20 mL deionized (DI) water under magnetic stirring for 30 min. Afterward, a piece of carbon cloth (CC) was socked in the mixture and then transferred into a Teflon-lined stainless-steel autoclave at 180 ℃ for 30 h. Then, the obtained products were cleaned with distilled (DI) water and ethanol successively. The product was dried in a vacuum oven at 60 °C for 10 h. Finally, the sample was calcinated at 300 °C for 2 h under Ar gas flow. The sample loading on CC ≈ 2.1 mg cm^{-2}. The same fabrication process was used to synthesize pure MoS_2 and other Re-SA/MoS_2 catalysts by using different molar ratios of Re and Mo ions.

Materials characterizations

Field emission scanning electron microscopy (FESEM, Hitachi S4800, Japan) was used to measure the morphology of the as-synthesized products. The microstructure and quantitative elemental analyses were tested on a JEOL-2100F microscope (JEOL, Japan) equipped with an energy-dispersive X-ray spectrometer (EDS). Aberration-corrected high-angle annular dark-field scanning transmission electron microscopy (HAADF-STEM) images and elemental maps of the Re-SA/MoS_2 catalysts were acquired on an aberration-corrected JEM-ARM-300F (JEOL, Japan) microscope operating at 300 kV. The phase structure of the catalysts was investigated by a Powder X-ray diffraction (XRD, Bruker AXSD8 Advance, Germany). The X-ray photoelectron spectroscopy (XPS, ThermoFisher Scientific, UK) data were collected on a VGESCALABMKII X-ray photoelectron spectrometer equipped with a non-monochromatized Al-Kα X-ray source, which was used to study the possible elemental composition of the samples and their chemical states within the materials. Re L_3-edge and Mo *K*-edge X-ray absorption spectroscopy (XAS) data were recorded in fluorescence mode at Beijing Synchrotron Radiation Facility.

Electrochemical measurements

The electrochemical measurements were performed by the electrochemical workstation (VMP3, Biologic Science Instruments, France; CHI 760e, CH Instrument, China). Saturated calomel and graphite rod electrodes were used as the reference and counter electrodes, respectively. The as-prepared Re-SA/MoS_2 electrocatalysts were utilized as the working electrode. The HER catalytic activity was examined by

measuring polarization curves with linear sweep voltammetry (LSV) at a scan rate of 5 mV s^{-1} in 1.0 M KOH and 0.5 M H_2SO_4 aqueous solutions, respectively. A potential conversion vs. RHE was calculated as follows:

$$E_{(RHE)} = E_{(Hg_2Cl_2/Hg)} + E^0_{(Hg_2Cl_2/Hg)} + 0.059 \times pH \quad (1)$$

where $E_{(RHE)}$ is the converted potential vs. RHE, $E_{(Hg_2Cl_2/Hg)}$ is the potential experimentally measured against the Hg_2Cl_2/Hg reference electrode and $E^0_{(Hg_2Cl_2/Hg)}$ is the standard potential of Hg_2Cl_2/Hg at 25 °C (0.241V).

To prepare the Pt/C electrode, the catalyst ink was prepared by ultrasonically dispersing the catalyst (5.0 mg) in a solution containing 1 mL of ethanol-DI water (1:3 vol) and 500 μL of 5 wt. % Nafion solution (117 solution, Aldrich). Then the ink was dropped onto the CC to yield a mass density equivalent to Re-SA/MoS_2 on CC. The cyclic voltammetry (CV) was performed at different scan rates (from 10 to 200 mV s^{-1}) to assess the electrochemically active surface area of the samples. The performance with *iR* compensation (95%) was obtained automatically from the electrochemical potentiostat. The electrochemical impedance spectroscopy (EIS) was tested at the frequency of 0.1 to 100 kHz to measure the charge transfer resistance. The cycling stability of the catalysts was conducted using a chronopotentiometry method both in acid (under the applied potential of -0.28 V) and alkaline (under the applied potential of -1.05 V) media.

Density functional theory method

We employed the VASP[1-2] to perform all the density functional theory (DFT) calculations within the generalized gradient approximation (GGA) using the Perdew-Burke-Ernzerhof (PBE)[3] formulation. We chose the projected augmented wave (PAW) potentials[4] to describe the ionic cores. Take valence electrons into account using a plane wave basis set with a kinetic energy cutoff of 450 eV. Partial occupancies of the Kohn-Sham orbitals were allowed using the Gaussian smearing method and a width of 0.05 eV. The electronic energy was considered self-consistent when the energy change was smaller than 10^{-5} eV. A geometry optimization was considered convergent when the force change was smaller than 0.05 eV/Å. The Brillouin zone is sampled with 3 × 3 × 1 Monkhorst mesh.[5]

The adsorption of hydrogen on the surface was calculated as follows:

$$\Delta G_{H^*} = E\,(slab + H^*) - E\,(slab) - 1/2E\,(H_2) + \Delta E\,(ZPE) - T\Delta S \quad (2)$$

Where E (slab + H*) is the total energy for the adsorption H, E (slab) is the energy of the pure surface, and E (H_2) is the energy of H_2 in the gas phase. ΔE (ZPE) is the zero-point energy change, and ΔS is the entropy change.

A constant of 0.24 eV corrected the Gibbs free energy calculation at 298 K as:

$$\Delta G_{H^*} = E\,(slab + H^*) - E\,(slab)1/2E\,(H_2) + 0.24 \quad (3)$$

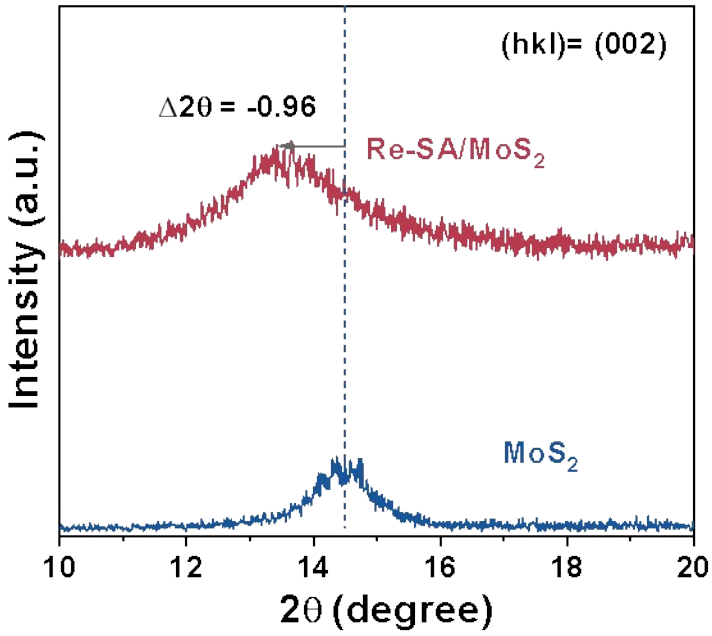

Fig. S1 Enlarged XRD patterns of the (002) peak of the fabricated samples.

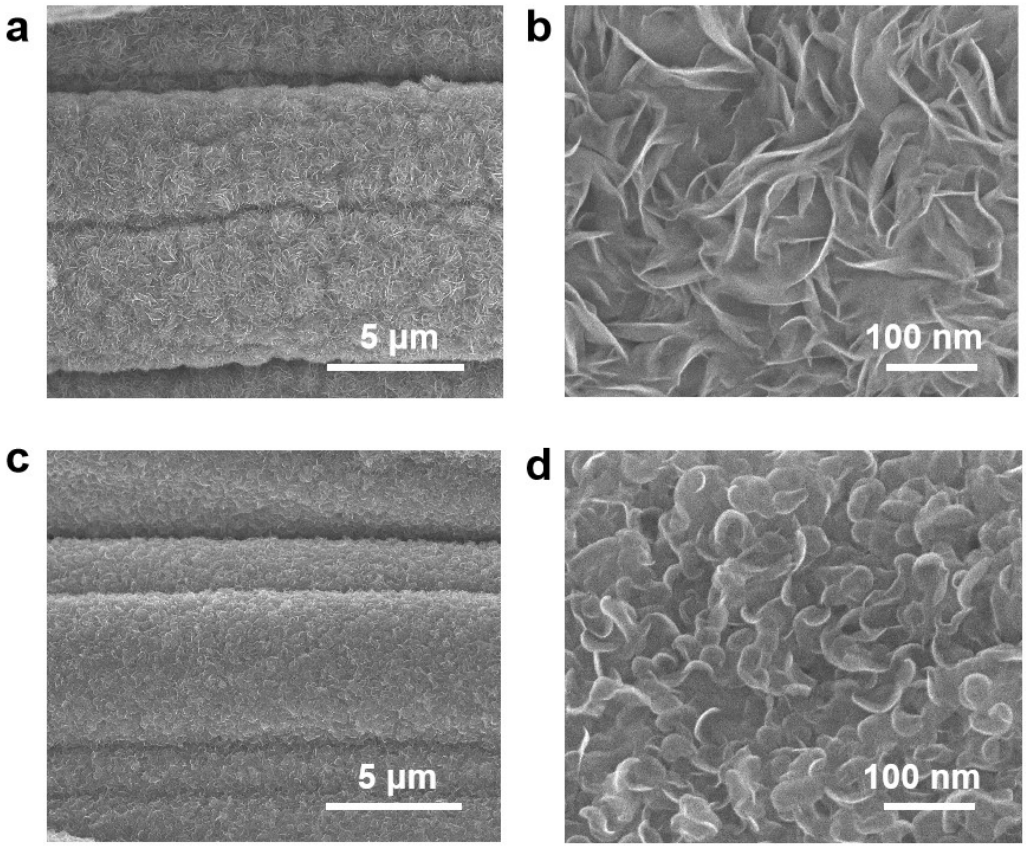

Fig. S2 SEM images of (a,b) MoS_2, and (c,d) Re-SA/MoS_2.

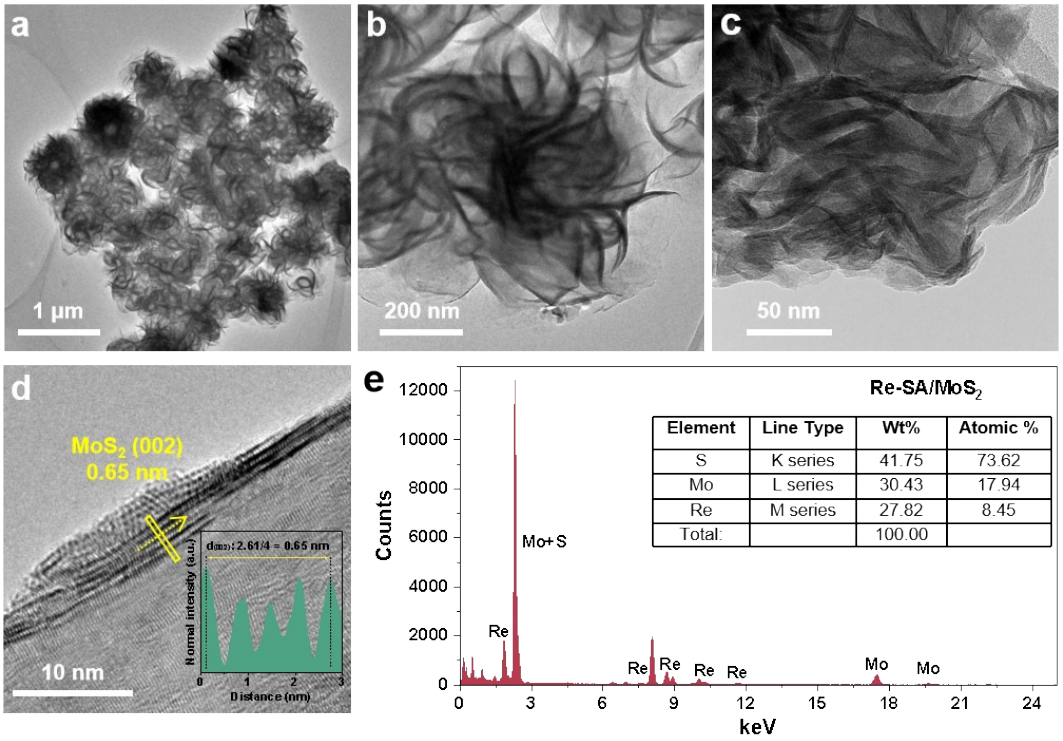

Fig. S3 (a,b) TEM image of the pure MoS_2 catalyst. (c) TEM image of Re-SA/MoS_2 catalyst. (d) HRTEM image of the pure MoS_2 catalyst. (e) EDS spectrum and the corresponding element contents of Re-SA/MoS_2.

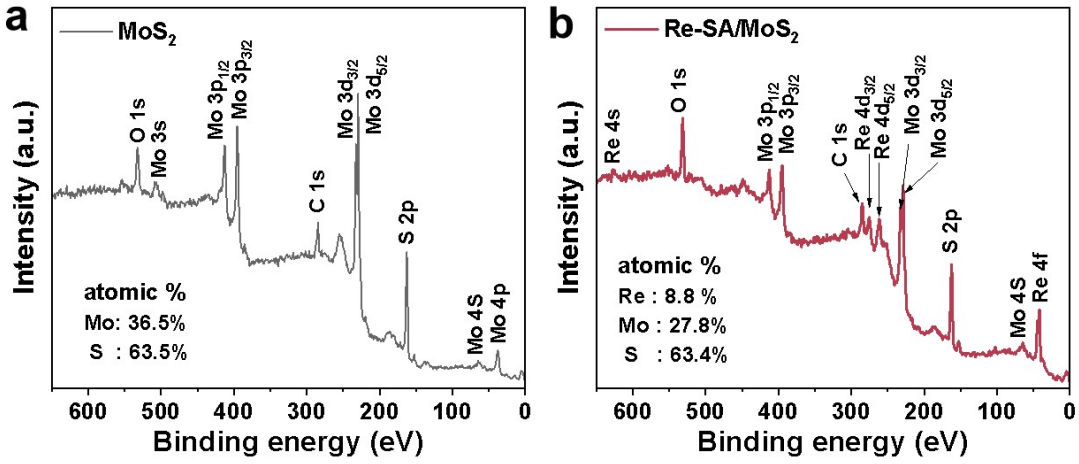

Fig. S4 (a,b) Full XPS spectra of the pure MoS_2 and Re-SA/MoS_2 catalysts.

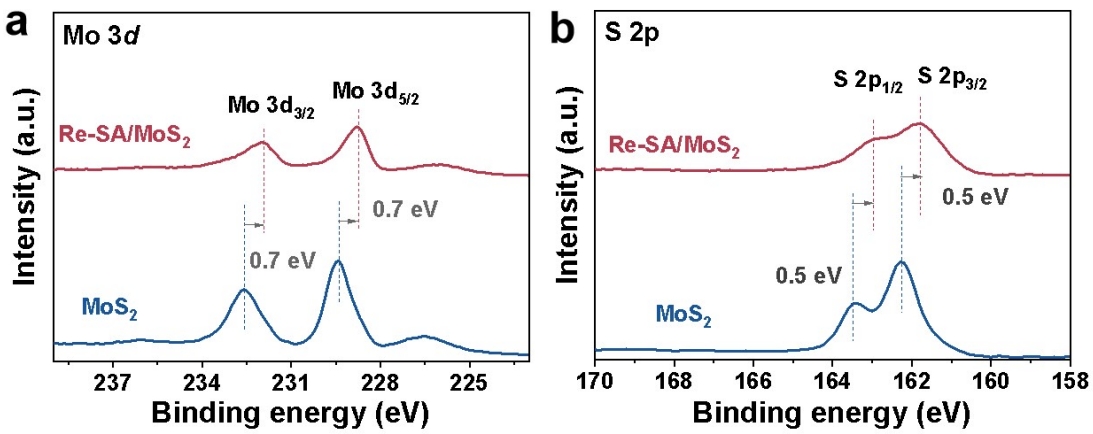

Fig. S5 (a) High-resolution Mo 3d core-level XPS spectra of the pure MoS_2 and Re-SA/MoS_2 catalysts. (b) High-resolution S 2p core-level XPS spectra of the pure MoS_2 and Re-SA/MoS_2 catalysts.

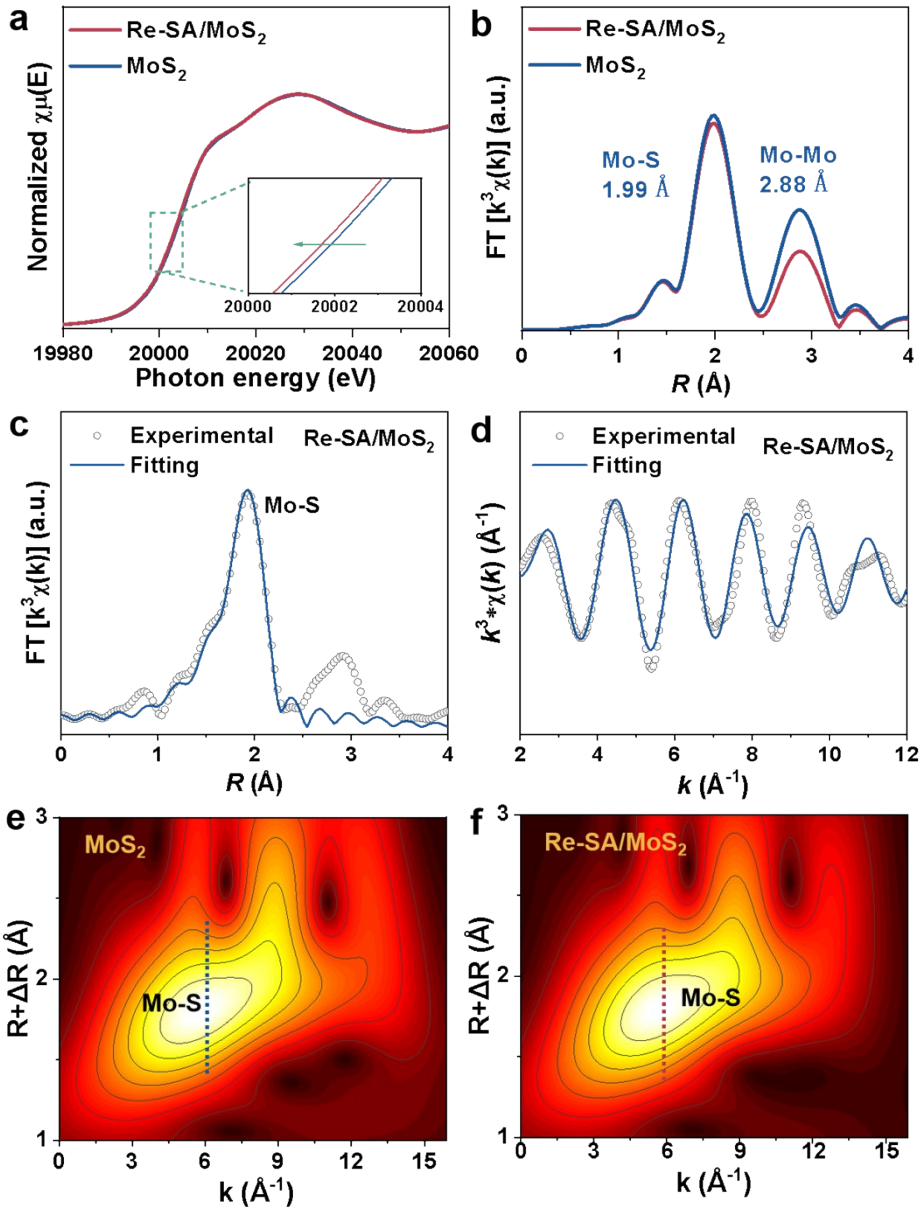

Fig. S6 (a) XANES spectra of Mo *K*-edge of the MoS_2 and Re-SA/MoS_2 catalysts. (b) EXAFS spectra of Fourier-transformed Mo *K*-edge of the MoS_2 and Re-SA/MoS_2 catalysts. (c) Mo *K*-edge EXAFS fitting results for Re-SA/MoS_2 in *R* space. (d) Mo *K*-edge EXAFS fitting results for Re-SA/MoS_2 in *k* space. (e,f) Wavelet transformation for Mo *K*-edge of MoS_2 and Re-SA/MoS_2 in *R* space.

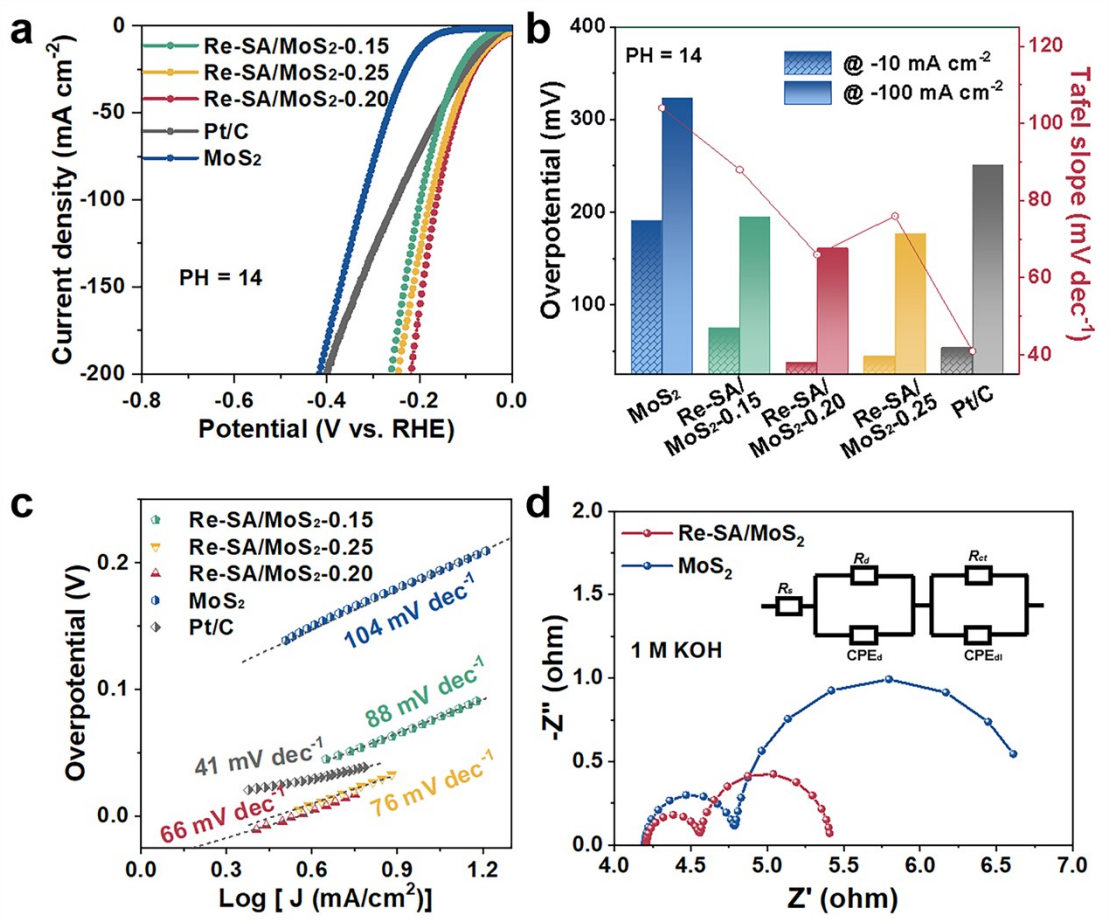

Fig. S7 HER performances of the Re-SA/MoS_2 electrocatalysts and control samples in H_2-saturated 1.0 M KOH: (a) LSV curves, (b) Overpotentials (left y-axis) at current densities of -10 and -100 mA cm^{-2}, and (c) Tafel plots (right y-axis). (d) EIS spectra of the fabricated catalysts in 1.0 M KOH.

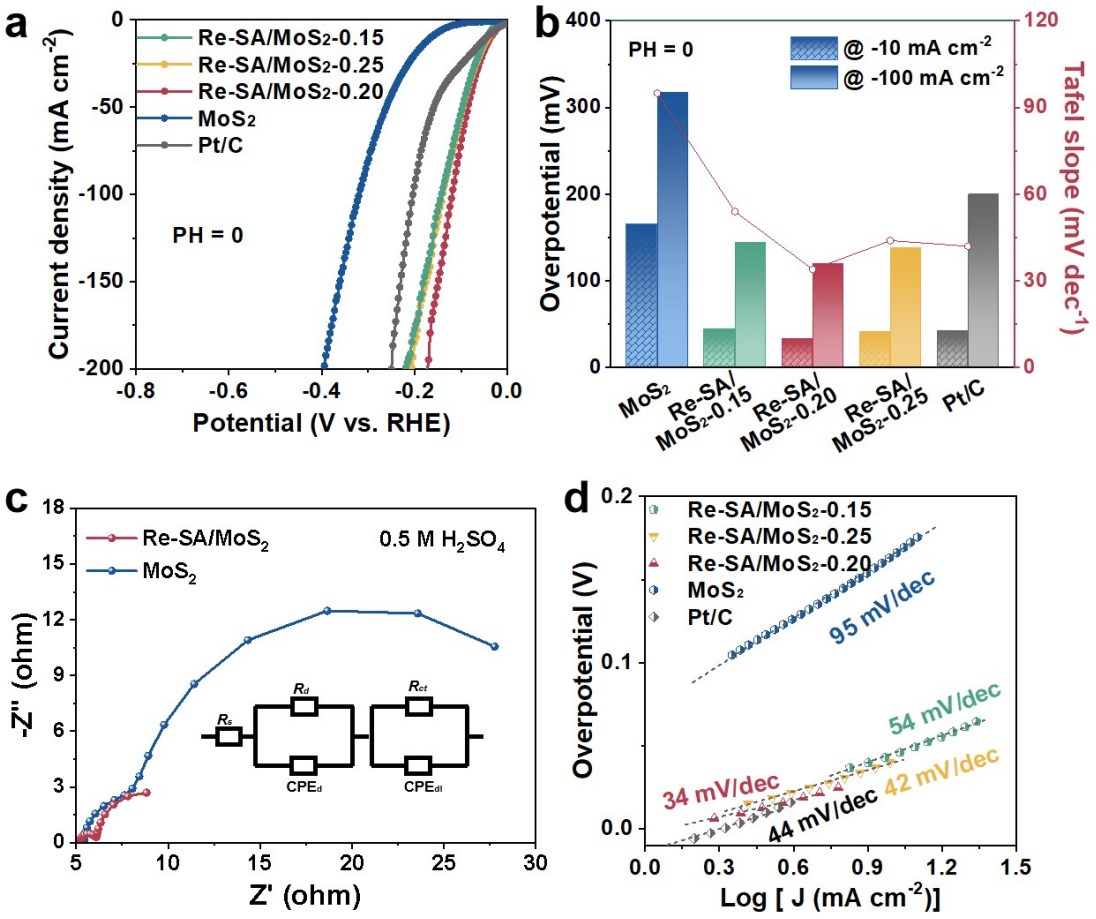

Fig. S8 HER performances of the Re-SA/MoS_2 electrocatalysts and control samples in H_2-saturated 0.5 M H_2SO_4: (a) LSV curves, (b) Overpotentials (left y-axis) at current densities of -10 and -100 mA cm^{-2}. (c) EIS spectra and (d) Tafel plots of the fabricated catalysts in 0.5 M H_2SO_4.

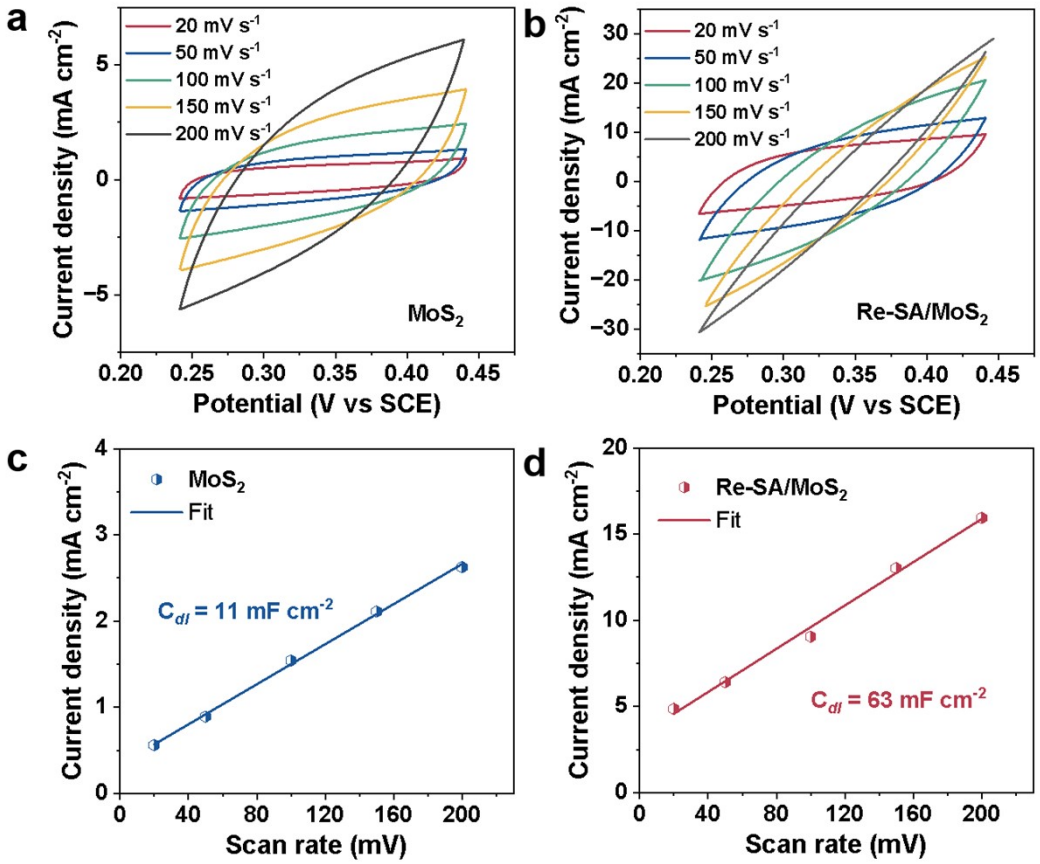

Fig. S9 Cyclic voltammograms of (a) MoS_2 and (b) Re-SA/MoS_2 at different rates ranging from 20-200 mV s^{-1} in the potential region from 0.24-0.44 V vs RHE. (c,d) Plots of capacitive current density at 0.29V versus scan rate, the corresponding slope can be used for determining the electrochemically accessible surface area of MoS_2 and Re-SA/MoS_2.

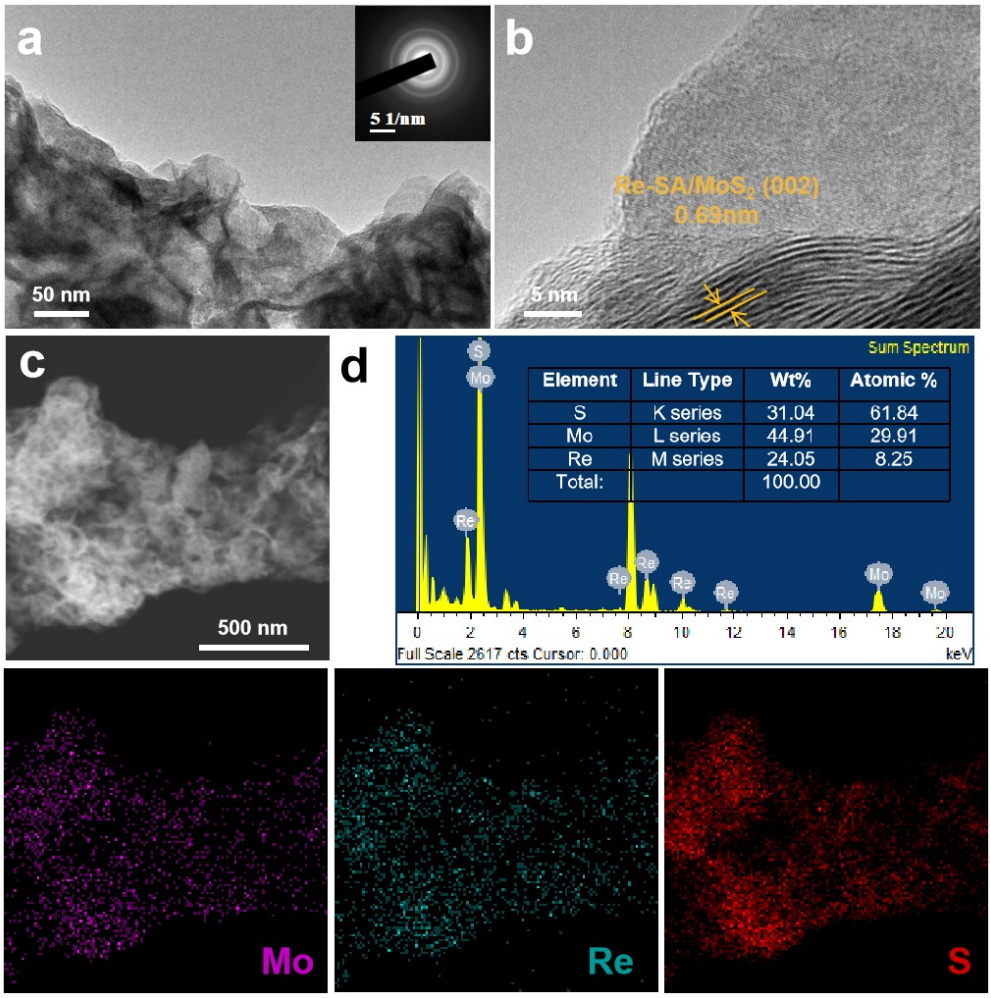

Fig. S10 (a) TEM image, (b) HRTEM image, and (c,d) EDS element mapping images and their corresponding contents of the Re-SA/MoS_2 catalysts after a long-term test for HER in 1.0 M KOH.

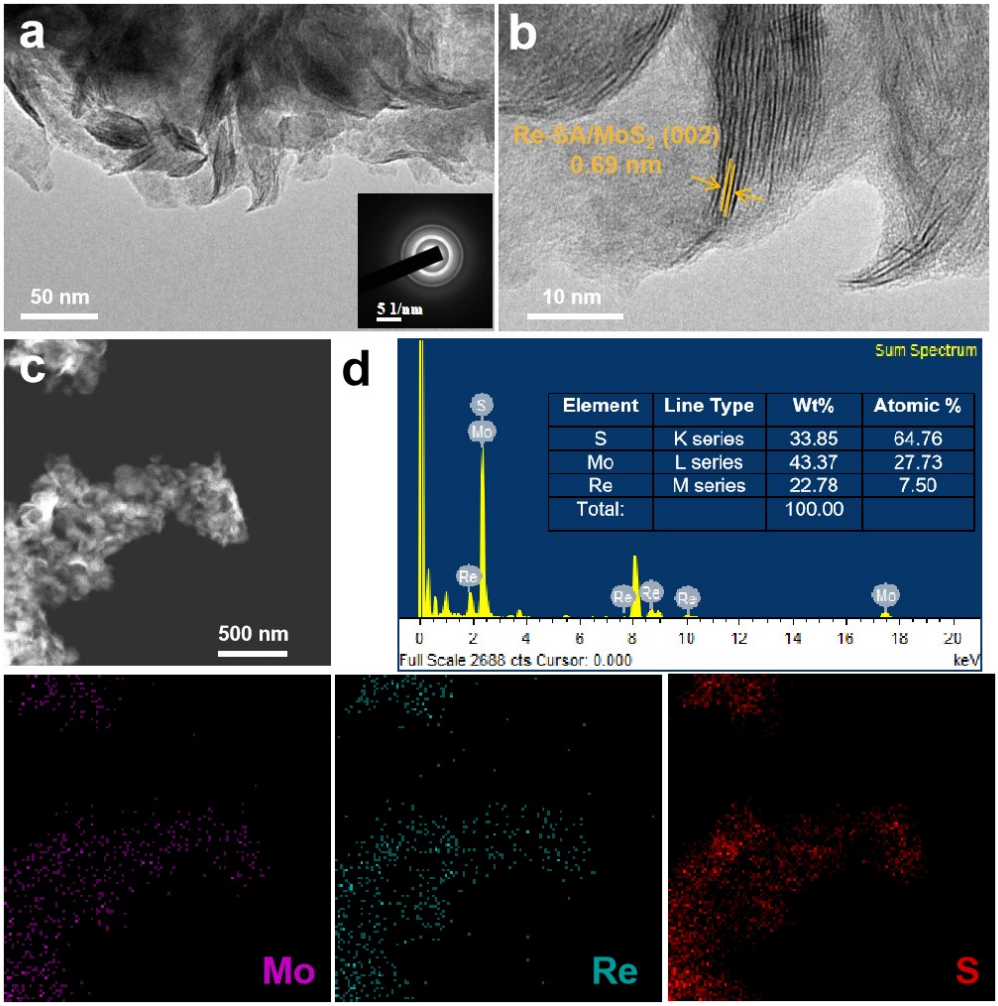

Fig. S11 (a) TEM image, (b) HRTEM image, and (c,d) EDS element mapping images and their corresponding contents of the Re-SA/MoS_2 catalysts after a long-term test for HER in 0.5 M H_2SO_4.

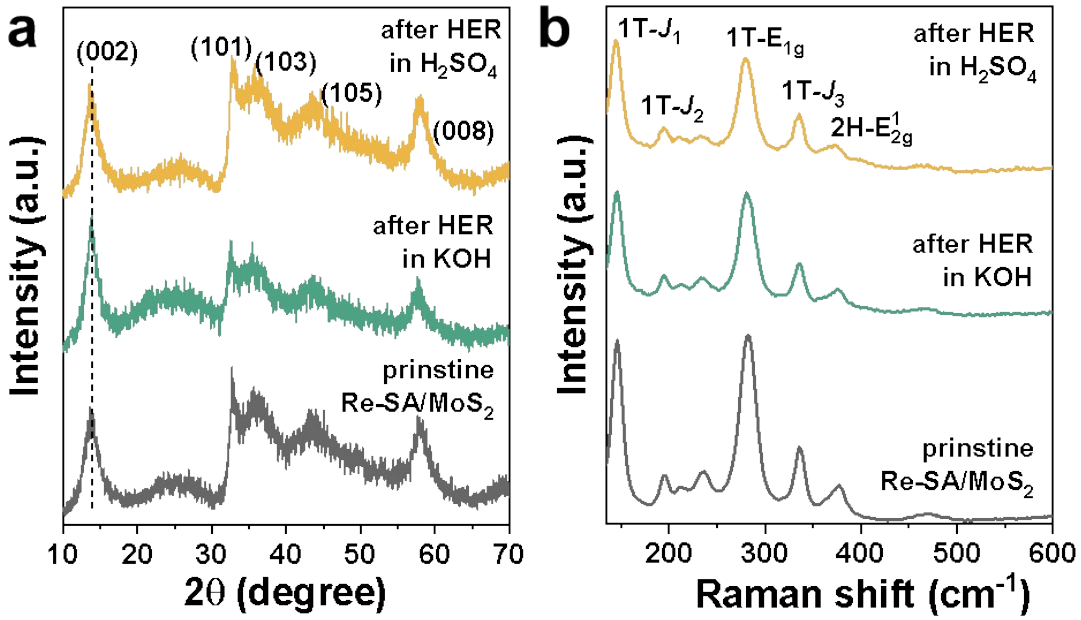

Fig. S12 XRD patterns (a) and Raman spectra (b) of the Re-SA/MoS_2 catalysts after a long-term test for HER in 1.0 M KOH and 0.5 M H_2SO_4.

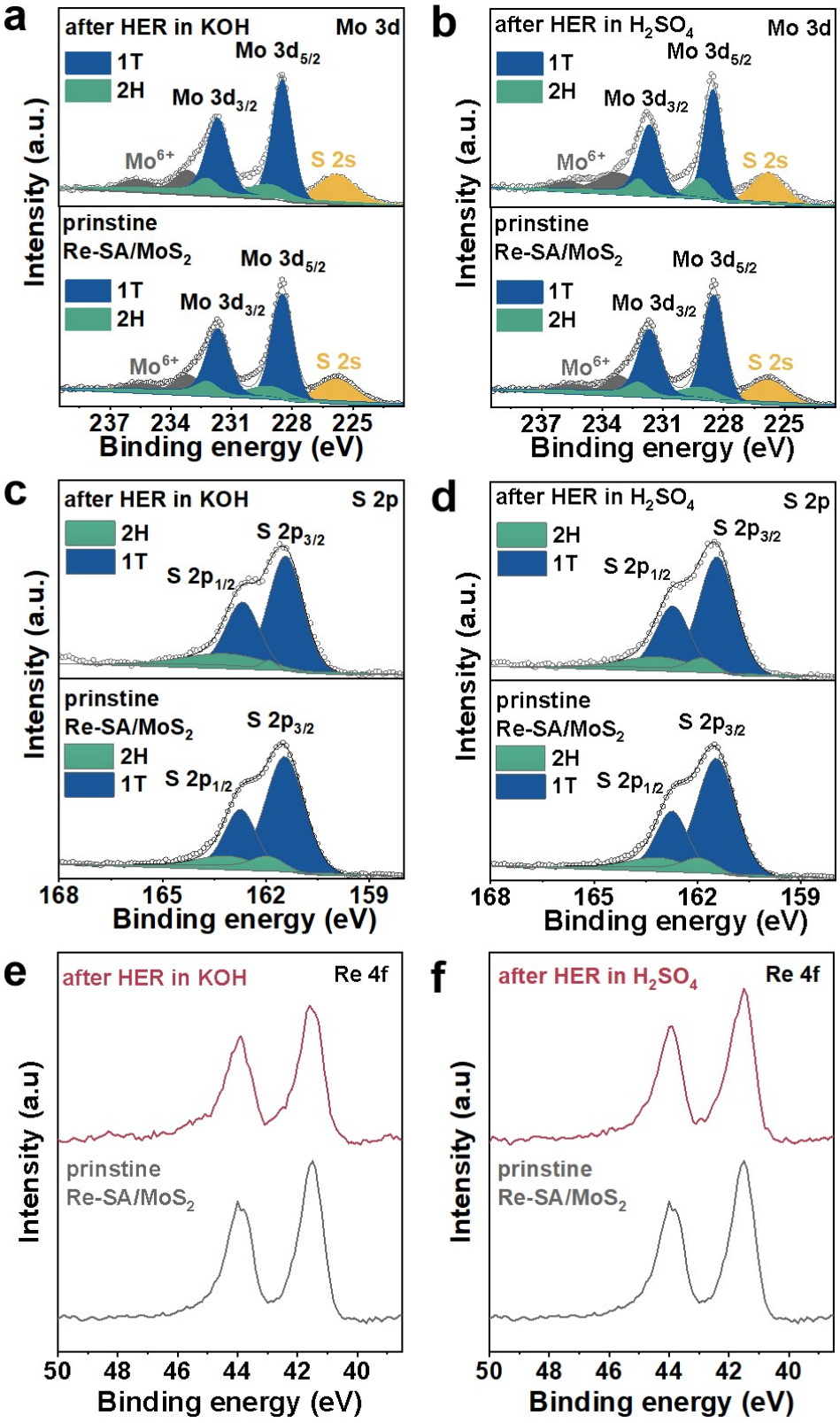

Fig. S13 XPS spectra of (a,b) Mo 3d, (c,d) S 2p and (e,f) Re 4f of the Re-SA/MoS_2 catalysts after a long-term test for HER in 1.0 M KOH and 0.5 M H_2SO_4.

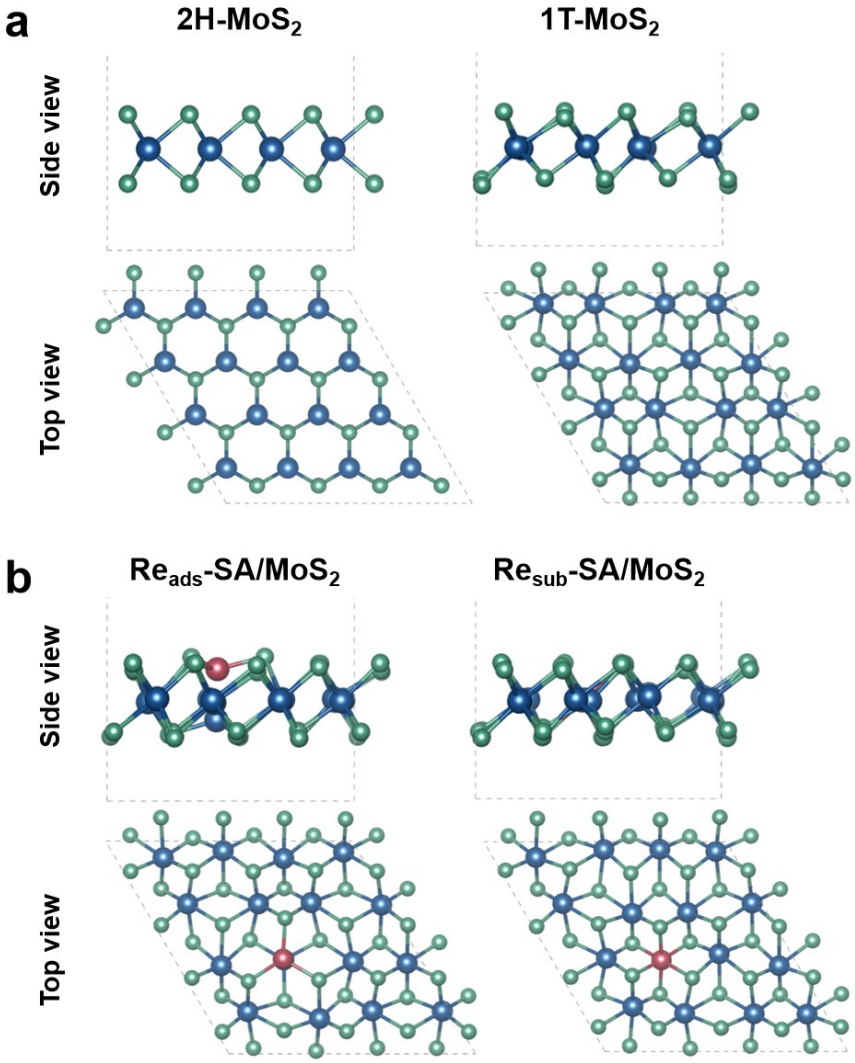

Fig. S14 (a) Constructed DFT model (side and top view) of 2H-MoS_2 and 1T-MoS_2. (b) Constructed DFT model (side and top view) of Re_{ads}-SA/MoS_2 and Re_{sub}-SA/MoS_2.

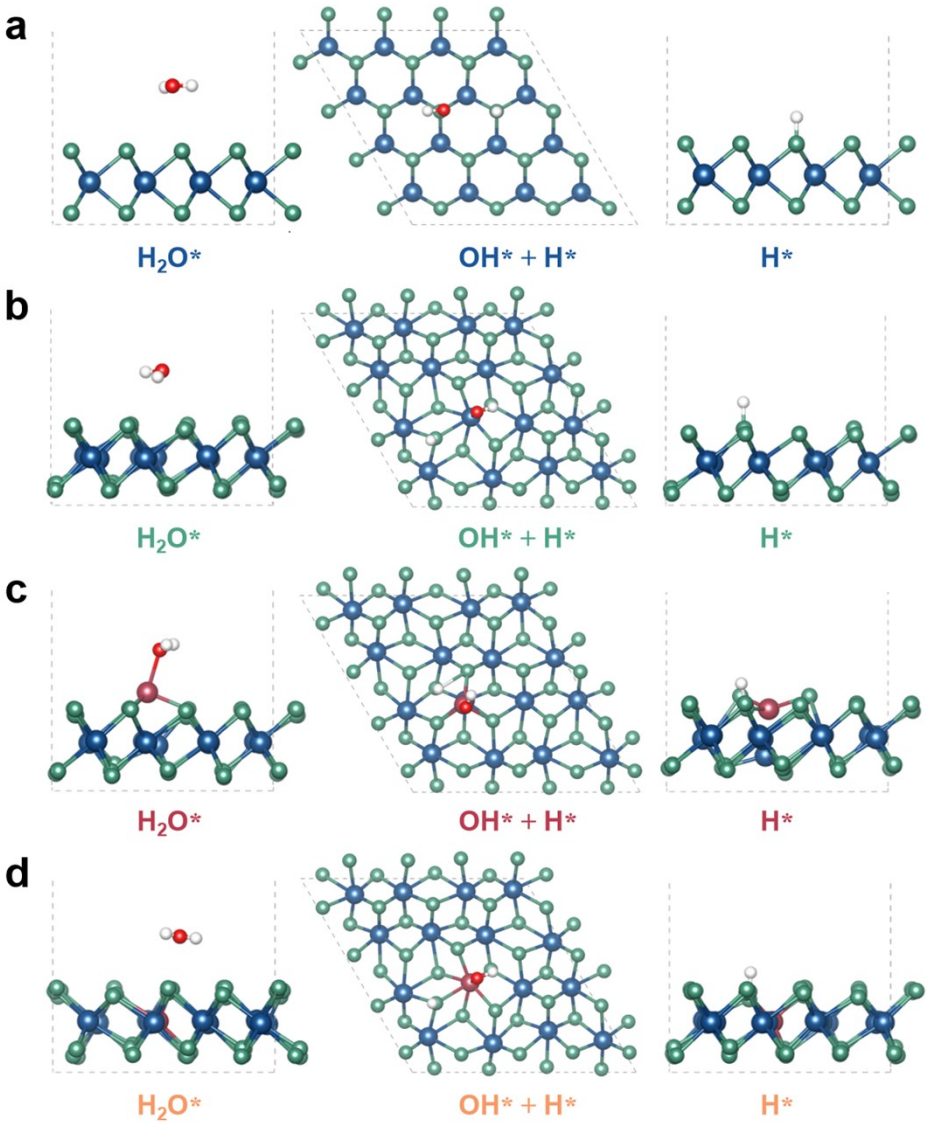

Fig. S15 Constructed DFT analysis for HER in adsorption of H_2O*, OH*+H*, and H* of t2H-MoS_2, 1T-MoS_2, Re_{ads}-SA/MoS_2 and Re_{sub}-SA/MoS_2.

Table S1 The fitting results of Re L_3-edge EXAFS spectra at *R* space for Re-SA/MoS_2 and reference samples.

	Path	N	R (Å)	σ^2 (×10^{-3} Å^2)	$\Delta E0$ (eV)	*R*, %
ReS_2[a]	Re-S	4.1±0.2	2.38±0.01	5±1	8.3±0.6	0.50
	Re-Re	2.0±0.1	2.79±0.01	4±1		
Re foil[b]	Re-Re	**12.0**	2.75	3±0.2	8.4±0.5	0.50
Re-SA/MoS_2[c]	Re-S	4.9±0.2	2.37±0.01	3±0.1	6.4±0.9	2.00

Note: N is the coordination number, R is the bond length, and σ^2 is the Debye-Waller factor. [a]: k range: 3-14 (Å^{-1}); R range: 1-3.0 Å; [b]: k range: 3-14 (Å^{-1}); R range: 1-3.1 Å; [c]: k range: 3-12.9 (Å^{-1}); R range: 1.0-2.3 Å; S_0^2 = 0.98, S_0^2 is determined from ReS_2. The bold numbers were set as fixed coordination numbers.

Table S2 The fitting result of Mo K-edge EXAFS spectra at *R* space for Re-SA/MoS_2 and reference sample.

Sample	Path	N	R (Å)	σ^2 (×10^{-3} Å^2)	$\Delta E0$ (eV)	*R*, %
MoS_2[a]	Mo-S	**6.0**	2.40±0.01	3±0.1	1.0±0.8	1.58
Re-SA/MoS_2[b]	Mo-S	5.9±0.2	2.40±0.01	3±0.1	0.8±0.7	0.81

Note: N is the coordination number, R is the bond length, and σ^2 is the Debye-Waller factor. [a]: k range: 3-13.5 (Å^{-1}); R range: 1-2.4 Å; [b]: k range: 3-13.6 (Å^{-1}); R range: 1.0-2.4 Å; S_0^2 = 0.74, S_0^2 is determined from MoS_2. The bold numbers were set as fixed coordination numbers.

Table S3 Comparison of the HER activity with reported MoS_2-based electrocatalysts in alkaline media.

Electrocatalysts	Electrolyte	Overpotential at 10 mA cm^{-2} (mV)	References
Re-SA/MoS_2	**1.0 M KOH**	**38**	**This work**
Ir/MoS_2	1.0 M KOH	44	ACS Energy Lett., 2019, 4, 368-374
Pd, Ru-$MoS_{2-x}OH_y$	1.0 M KOH	48	Nat. Commun., 2020, 11, 1116
Pt-SAs/MoS_2	1.0 M KOH	65	Nat. Commun., 2021, 12, 3021
Ni_3S_2@MoS_2	1.0 M KOH	78.1	Adv. Mater., 2022, 34, 2202195
$1T_{0.81}MoS_2$@Ni_2P	1.0 M KOH	95	Nat. Commun., 2021, 12, 5260
MoS_2/NiFe-LDH	1.0 M KOH	110	Nano Lett., 2019, 19, 4518-4526
MoS_2-C	1.0 M KOH	155	Adv. Energy Mater., 2019, 9, 1802553
MoS_2@Au	1.0 M KOH	176	Nat. Commun., 2019, 10, 1348
1T-MoS_2	1.0 M KOH	250	Adv. Mater., 2020, 32, 2001889

Table S4 The detailed information on the EIS results of the fabricated catalysts in 1.0 M KOH.

Content	MoS_2	Re-SA/MoS_2
R_s (solution resistance)	5.32 Ω	4.15 Ω
R_d (diffusion resistance)	0.59 Ω	0.85 Ω
R_{ct} (charge transfer resistance)	2.00 Ω	0.35 Ω

Table S5 Comparison of the HER activity with reported MoS_2-based electrocatalysts in acid media.

Electrocatalysts	Electrolyte	Overpotential at 10 mA cm^{-2} (mV)	References
Re-SA/MoS_2	**0.5 M H_2SO_4**	**34**	**This work**
N, Pt-MoS_2	0.5 M H_2SO_4	38	Energy Environ. Sci., 2022, 15, 1201-1210
Pd, Ru-$MoS_{2-x}OH_y$	0.5 M H_2SO_4	45	Nat. Commun., 2020, 11, 1116
Co, Pd-MoS_2	0.5 M H_2SO_4	49.3	Adv. Mater., 2020, 32, 2001167
Pt-SAs/MoS_2	0.5 M H_2SO_4	59	Nat. Commun., 2021, 12, 3021
Rh-MoS_2	0.5 M H_2SO_4	67	Angew. Chem. Int. Ed., 2020, 59, 10502-10507
Pd-MoS_2	0.5 M H_2SO_4	78	Nat. Commun., 2018, 9, 2120
Zn-MoS_2	0.5 M H_2SO_4	130	J. Am. Chem. Soc., 2017, 139, 15479-15485
Pd-1T-$^{S}MoS_2$	0.5 M H_2SO_4	140	ACS Catal., 2019, 9, 7527-7534
MoS_2@Au	0.5 M H_2SO_4	136	Nat. Commun., 2019, 10, 1348

Table S6 EIS results of the fabricated catalysts in 0.5 M H_2SO_4.

Content	MoS_2	Re-SA/MoS_2
R_s (solution resistance)	5.98 Ω	5.20 Ω
R_d (diffusion resistance)	2.86 Ω	0.91 Ω
R_{ct} (charge transfer resistance)	25.13 Ω	5.37 Ω

Supplementary references

1 G. Kresse and J. Furthmüller, *Phys. Rev. B*, 1996, **54**, 11169-11186.

2 G. Kresse and J. Furthmüller, *Comput. Mater. Sci.*, 1996, **6**, 15-50.

3 J. P. Perdew, K. Burke and M. Ernzerhof, *Phys. Rev. Lett.*, 1996, **77**, 3865-3868.

4 G. Kresse and D. Joubert, *Phys. Rev. B*, 1999, **59**, 1758-1775.

5 H. J. Monkhorst and J. D. Pack, *Phys. Rev. B*, 1976, **13**, 5188-5192.